Ann Neurol. Author manuscript; available in PMC 2017 March 01.

Published in final edited form as:
Ann Neurol. 2016 March ; 79(3): 354–365. doi:10.1002/ana.24570.

Activation of Specific Neuronal Networks Leads to Different Seizure Onset Types

Zahra Shiri, BSc[1], **Frédéric Manseau, PhD**[2], **Maxime Lévesque, PhD**[1], **Sylvain Williams, PhD**[2], and **Massimo Avoli, MD, PhD**[1]

[1]Montreal Neurological Institute, Department of Neurology and Neurosurgery, and Department of Physiology, McGill University, Montreal, Quebec, Canada

[2]Douglas Mental Health University Institute, McGill University, Montreal, Quebec, Canada

Abstract

Objective—Ictal events occurring in temporal lobe epilepsy patients and in experimental models mimicking this neurological disorder can be classified, based on their onset pattern, into low-voltage, fast versus hypersynchronous onset seizures. It has been suggested that the low-voltage, fast onset pattern is mainly contributed by interneuronal (γ-aminobutyric acidergic) signaling, whereas the hypersynchronous onset involves the activation of principal (glutamatergic) cells.

Methods—Here, we tested this hypothesis using the optogenetic control of parvalbumin-positive or somatostatin-positive interneurons and of calmodulin-dependent, protein kinase–positive, principal cells in the mouse entorhinal cortex in the in vitro 4-aminopyridine model of epileptiform synchronization.

Results—We found that during 4-aminopyridine application, both spontaneous seizure-like events and those induced by optogenetic activation of interneurons displayed low-voltage, fast onset patterns that were associated with a higher occurrence of ripples than of fast ripples. In contrast, seizures induced by the optogenetic activation of principal cells had a hypersynchronous onset pattern with fast ripple rates that were higher than those of ripples.

Interpretation—Our results firmly establish that under a similar experimental condition (ie, bath application of 4-aminopyridine), the initiation of low-voltage, fast and of hypersynchronous onset seizures in the entorhinal cortex depends on the preponderant involvement of interneuronal and principal cell networks, respectively.

Seizures in patients presenting with temporal lobe epilepsy (TLE) are mainly characterized by 2 distinct electrographic onset patterns, defined as low-voltage, fast (LVF) and hypersynchronous (HYP).[1,2] LVF seizures are characterized at onset by the occurrence of a sentinel spike followed by low-amplitude, high-frequency activity, whereas the initiation of

Address correspondence to Dr Avoli, Montreal Neurological Institute, McGill University, 3801 University Street, Montreal, QC, Canada, H3A 2B4. massimo.avoli@mcgill.ca.

Author Contributions
Conception and design of the study: S.W., M.A. Acquisition and analysis of data: Z.S., F.M., M.L., M.A. Drafting the manuscript or figures: Z.S., F.M., M.L., S.W., M.A.

Potential Conflicts of Interest
Nothing to report.

HYP seizures coincides with a series of focal (so-called preictal) spiking at a frequency of approximately 2Hz.[3] LVF and HYP seizures may mirror the activity of distinct limbic structures.[4] Accordingly, Velasco et al[2] have reported that LVF seizures rest on the activity of hippocampal and parahippocampal networks, whereas HYP seizures originate from local circuits in the hippocampal formation. In addition, TLE patients presenting with HYP seizures have histopathological patterns of atrophy that are consistent with hippocampal sclerosis, whereas LVF seizures are linked to a more diffuse and bilateral distribution of atrophy.[1] Finally, in animal models of TLE, LVF seizures more often initiate in parahippocampal structures, whereas HYP seizure onset may be limited to the hippocampus.[5,6]

Recently, the analysis of high-frequency oscillations (HFOs; ripples: 80–200Hz, fast ripples: 250–500Hz) during spontaneous HYP and LVF seizures in the pilocarpine and kainic acid model of TLE has suggested that these 2 seizure onset patterns may rely on distinct mechanisms of initiation. LVF seizures were found to be mainly associated with HFOs in the ripple frequency range, thus suggesting the predominant involvement of interneuronal (inhibitory) networks; in contrast, HYP seizures were mostly accompanied by fast ripple occurrence, thus highlighting the potential role of principal (glutamatergic) networks.[6,7] Evidence obtained to date suggests that pathologic HFOs in the ripple band should represent population inhibitory postsynaptic potentials generated by principal neurons entrained by synchronously active interneuron networks, whereas those in the fast ripple band reflect the synchronous firing of abnormally active principal cells, and thus are not dependent on inhibitory processes.[8–10]

It has been demonstrated that 4-aminopyridine (4AP) application induces LVF onset discharges in several limbic and paralimbic structures maintained in vitro.[11] In addition, systemic injection of 4AP in vivo has been shown to induce LVF onset pattern seizures.[12,13] Finally, we have found that optogenetic activation of parvalbumin (PV)-positive interneurons of entorhinal cortex (EC) in a constitutive model of channelrhodopsin-2 (ChR2) expression leads to the initiation of in vitro LVF seizures in the limbic system.[14] Therefore, in this study, we aimed to test the hypothesis that distinct (ie, LVF and HYP) patterns of seizure onset rely on the activity of different neuronal networks in the in vitro 4AP model using the optogenetic control of PV-positive and somatostatin (SOM)-positive interneurons as well as of calmodulin-dependent protein kinase (CamKII)-positive principal cells in the EC of mice where an enhanced ChR2 opsin was transcranially, locally injected.

Materials and Methods

Animals

All procedures were performed according to protocols and guidelines of the Canadian Council on Animal Care (http://www.ccac.ca/en_/standards/guidelines) and were approved by the McGill University Animal Care Committee. PV-Cre (Jackson Laboratory, Bar Harbor, ME; B6;129P2-*Pvalb*$^{tm1[cre]Arbr}$/J, stock number 008069), SOM-Cre (Jackson Laboratory, *Ssttm2.1[cre]Zjh*/J, stock number 013044), and CamKII-Cre (Jackson Laboratory, B6.Cg-Tg[Camk2a-cre]T29-1Stl/J, stock number 005359) homozygote mouse colonies were bred and maintained in-house to generate pups that were used in this study.

Stereotaxic Virus Injections

Four PV-Cre, 7 SOM-Cre, and 8 CamKII-Cre male or female pups were anesthetized at postnatal day (P) 15 using isoflurane and positioned in a stereotaxic frame (Stoelting, Wood Dale, IL). AAVdj-ChETA-eYFP virus (UNC Vector Core, Chapel Hill, NC) was delivered in the EC (0.6 μl at a rate of 0.06 μl/min). Injection coordinates were: anteroposterior, −4.00mm from bregma; lateral, ±3.60mm; dorsoventral, −4.00mm. The transverse sinus was used as a point of reference, and the injection needle was inserted with a 2° anteroposterior angle. After completion of the surgery, pups were returned to their home cage.

Slice Preparation

Mice were deeply anesthetized with inhaled isoflurane and decapitated at P30 to P40. Brains were quickly removed and immersed in ice-cold slicing solution containing (in mM): 25.2 sucrose, 10 glucose, 26 $NaHCO_3$, 2.5 KCl, 1.25 KH_2PO_4, 4 $MgCl_2$, and 0.1 $CaCl_2$ (pH 7.3, oxygenated with 95% O_2/5% CO_2). Horizontal brain sections (thickness=400 μm) containing the EC were cut using a vibratome (VT1000S; Leica, Wetzlar, Germany) and incubated for 1 hour or more in a slice saver filled with artificial cerebrospinal fluid (ACSF) of the following composition (in mM): 125 NaCl, 25 glucose, 26 $NaHCO_3$, 2 KCl, 1.25 NaH_2PO_4, 2 $MgCl_2$, and 1.2 $CaCl_2$.

Electrophysiological Recordings and Photostimulation

Slices were transferred to a submerged chamber, where they were continuously perfused with oxygenated ACSF (KCl and $CaCl_2$ adjusted to 4.5 and 2mM, respectively; 30 °C, 10–15ml/min). Field potentials were recorded using ACSF-filled microelectrodes (1–2MΩ) positioned in the EC in the presence of 4AP. Signals were recorded with a differential alternating current amplifier (A-M Systems, Sequim, WA), filtered online (0.1–500Hz), digitized with a Digidata 1440a (Molecular Devices, Sunnyvale, CA), and sampled at 5kHz using pClamp software (Molecular Devices). In a subset of experiments, whole-cell patch-clamp recordings were performed on visually identified neurons from EC slices. Patch electrodes (2–3MΩ) were filled with a solution containing the following (in mM): 144 K-gluconate, 3 $MgCl_2$, 10 N-2-hydroxyethylpiperazine-N′-2-ethanesulfonic acid, 0.2 ethyleneglycoltetraacetic acid, 2 Na_2ATP, and 0.3 guanosine triphosphate, pH7.3 (285–295mOsm). Signals were amplified using a Multiclamp 700B patch-clamp amplifier (Molecular Devices), sampled at 20kHz, and filtered at 10kHz.

For ChR2 excitation, blue light (473nm, intensity=35mW) was delivered through a custom-made light-emitting diode (LED) system, where the LED (Luxeon Star LEDs, Brantford, Ontario, Canada) was coupled to a 3mm- or 1mm-wide fiber-optic for field or whole-cell recording experiments, respectively (Edmund Optics, Barrington, NJ), and was placed above the recording region. For optogenetic activation of PV- and SOM-positive interneurons, light pulses (1-second duration) were delivered at 0.2Hz for 30 seconds with a 150-second interval between trains. For optogenetic activation of CamKII-positive principal cells, light pulses (20-millisecond duration) were delivered at 2Hz for 30 seconds with a 150-second interval between trains. All reagents were obtained from Sigma-Aldrich (St Louis, MO) and were bath applied.

Analysis of HFOs

Field potentials were first low-pass filtered at 500Hz and then downsampled to 2,000Hz. For each ictal discharge, raw field potential signals were band-pass filtered in the 80 to 200Hz and in the 250 to 500Hz frequency ranges for identification of ripples and fast ripples, respectively; a more thorough description of this procedure is provided in Salami et al.[13] Rates of ripples and fast ripples were computed using average values obtained from 10 ictal discharges per plot. The ictal period was arbitrarily divided into 3 equal parts, and rates of ripples and fast ripples in each part were compared using nonparametric Wilcoxon rank sum tests followed by Bonferroni–Holm corrections for multiple comparisons. This allowed us to evaluate whether ripples or fast ripples predominated at specific moments of the ictal period. Statistical tests were performed in MATLAB 7.11.0 (MathWorks, Natick, MA) using the Statistics Toolbox. The level of significance was set to $p<0.05$.

Results

Optogenetic Activation of PV-Positive Interneurons Leads to LVF Onset Seizures

We analyzed a total of 182 ictal events recorded from the EC of PV-Cre mice transcranially injected with the enhanced ChR2 opsin, ChETA (n=6 slices). Of these events, 142 occurred spontaneously and 40 were triggered using a 30-second train of 1-second light pulses at 0.2Hz. Representative examples of spontaneous and light-triggered events are shown in Figure 1. When the onset of a spontaneous ictal-like event was expanded, an LVF onset pattern consistently initiated by an isolated spike became evident. A similar LVF onset pattern was observed when the ictal events were triggered by optogenetic activation of PV interneurons. Spontaneously occurring events lasted 47.74±1.34 seconds, a duration that was similar to what was found for the optogenetically induced events (ie, 45.57±2.23 seconds). However, spontaneous ictal discharges occurred every 156.61±9.81 seconds, while during optogenetic PV-cell stimulation we could reduce their interval of occurrence to 138.13±4.89 seconds ($p<0.05$).

As shown in Figure 2, we also performed patch-clamp recordings of fast-spiking, PV-positive interneurons in the whole-cell mode (n=3). First, we characterized the patched cell by injecting intracellular depolarizing current pulses to reveal the typical firing activity of a fast-spiking PV-positive interneuron.[15] These interneurons reliably responded to optogenetic stimulation over time. Moreover, as illustrated in Figure 2C (see also expanded trace), fast-spiking PV-positive interneurons generated a barrage of action potentials (delay of initial depolarization=5.43±0.51 milliseconds; average spike frequency=155.68±10.99Hz; average duration of barrage=0.83±0.06 seconds) in response to the optogenetic stimulus as well as in coincidence with the initial spike; then, they depolarized progressively, undergoing a “firing depolarizing block” during the initial part of the LVF ictal discharge (n=11 events). Later, during the subsequent “tonic” electrographic phase of the ictal discharge, these interneurons could resume action potential firing that occurred synchronously with each “clonic” field potential transient.

To ensure that the responses evoked by optogenetic stimuli were dependent on the release of γ-aminobutyric acid (GABA) subsequent to interneuron discharge, we simultaneously

blocked $GABA_A$ and $GABA_B$ receptors using picrotoxin (50 μM) and CGP55845 (4 μM), respectively. Under these pharmacological conditions, all spontaneous and stimulated ictal-like events as well as light-induced interictal events were abolished (n=3 slices; data not shown, but see Shiri et al[14].

Optogenetic Activation of SOM-Positive Interneurons Leads to LVF Onset Seizures

Next, we established whether the ability of interneuron activation to drive ictal discharges is linked exclusively to fast-spiking interneurons, or whether ictal discharges could also be triggered by activating regular-spiking SOM-positive interneurons. We analyzed a total of 224 ictal discharges recorded from the EC of SOM-Cre mice that had been transcranially injected with ChETA (n=11 slices). Of these events, 170 occurred spontaneously and 54 were stimulated by a 30-second train of 1-second light pulses at 0.2Hz; this protocol was similar to that employed in the PV-positive interneuron experiments. As illustrated in Figure 3 (A, arrow), the onset of an expanded spontaneous ictal-like event was characterized, in these experiments as well, by the occurrence of an isolated spike leading to an LVF onset pattern. Interestingly, the same pattern of field activity occurred at the onset of ictal events when they were triggered by activation of SOM interneurons. In these experiments, spontaneous ictal discharges lasted 64.39±1.86 seconds and optogenetically induced events had durations of 60.52±2.30 seconds. Spontaneous ictal discharges occurred regularly (every 130.31±6.35 seconds) but could be driven at a more frequent rate during optogenetic stimulation of SOM cells, that is, every 105.42±5.51 seconds ($p<0.05$). In these experiments as well, concomitant application of $GABA_A$ and $GABA_B$ receptor antagonists abolished all spontaneous and induced ictal-like events (n=3 slices). Under these conditions, presumptive glutamatergic field bursts occurred for the entire length of the recording but did not appear to follow the stimulation pattern (see expanded region in Fig 3E).

Optogenetic Activation of CamKII-Positive Principal Cells Leads to HYP Onset Seizures

In this set of experiments, we analyzed a total of 293 ictal events that were recorded from the EC of brain slices expressing ChETA in CamKII-positive principal cells (n=14 slices). Of these ictal discharges, 141 occurred spontaneously whereas 152 events were triggered by a 30-second train of 20-milliseconds light pulses at 2Hz. Representative examples of spontaneous and light-triggered events are shown in Figure 4. When the onset of a spontaneous ictal event was expanded, an LVF onset—which was preceded by a typical isolated spike—could be identified. In contrast, the onset of ictal discharges triggered by principal cell activation was characterized by repeated spiking and thus resembled a HYP onset pattern. We found that spontaneous ictal discharges lasted 44.95±1.82 seconds, whereas those induced by light pulses were significantly shorter (37.07±0.72 seconds; $p<0.01$). During 4AP application, ictal discharges occurred spontaneously every 121.16±6.49 seconds but were driven at higher frequency by light stimulation (ie, 111.23±1.70 seconds; $p<0.05$).

CamKII-positive cells were also recorded in the whole-cell mode (n=5) to analyze their electrophysiological properties, their responses to light stimuli, and their activity during ictal discharges. As illustrated in Figure 5A, these neurons responded to injection of depolarizing current pulses by generating repetitive action potential firing with some degree of

adaptation, as reported for regular-spiking, principal cells in the EC_{16} and in several cortical structures.[17,18] We also found that these recorded neurons reliably responded to optogenetic stimulation with a short burst of action potentials when tested at different time points during the experiment (delay of initial depolarization=6.37±0.14 milliseconds). In the absence of optogenetic stimulation, spontaneous, 4AP-induced ictal events with LVF onset patterns in the field recording were characterized intracellularly by a period of action potential quiescence at ictal onset, whereas firing resumed during the late tonic phase of the discharge (n=12 events). In contrast, as illustrated in Figure 5D, principal cell firing occurred in coincidence with the preictal spikes that were characteristic of optogenetically induced HYP onset ictal discharges (duration of bursts=0.27 seconds; n=15 events; see expanded onset).

To further establish the contribution of principal glutamatergic cells to the evoked discharges, we simultaneously blocked the N-methyl-D-aspartate (NMDA) and non-NMDA receptors using 3-([*R*]-2-carboxypiperazin-4-yl)-propyl-1-phosphonic acid (CPP; 5 μM) and 6-cyano-7-nitroquinoxaline-2,3-dione (CNQX; 5 μM) in experiments in which we stimulated interneurons (n=3; Fig 6A) or principal cells (n=3; see Fig 6B). Under these conditions, all spontaneous and stimulated ictal events were abolished; however, interneuron stimulation continued to evoke presumably GABAergic discharges, whereas principal cell stimulation failed to induce such events. In the latter case, spontaneous GABAergic discharges could be recorded independently of the stimulation.

HFOs Associated with LVF and HYP Onset Seizures

Finally, we quantified the rate and pattern of HFO occurrence throughout the ictal discharges recorded in the EC (Fig 7). This analysis showed that ripple rates were higher than fast ripple rates ($p<0.01$) at the onset of all spontaneous LVF onset ictal events as reported for LVF seizures recorded in vivo in the pilocarpine model of TLE[6] and in the acute 4AP model.[13] A similar pattern of HFO distribution was associated with LVF onset seizures triggered by the activation of PV- and SOM-positive interneurons and interestingly, this pattern was still observed in 4AP-induced spontaneous LVF seizures in CamKII-Cre pups. These results therefore suggest that activation of interneuronal networks can trigger seizure like events resembling human LVF seizures. In contrast, ictal discharges triggered by the activation of principal cells revealed higher fast ripple rates at seizure onset ($p<0.01$) as reported to occur in HYP onset seizures occurring in vivo.[6,13]

Discussion

The main findings of our study can be summarized as follows: (1) spontaneous ictal events recorded in vitro from the EC during 4AP application are characterized by an LVF onset pattern; (2) similar LVF onset ictal discharges can be triggered by optical activation of PV- and SOM-positive interneurons; (3) in contrast, ictal discharges triggered by CamKII-pyramidal cell stimulation are associated with an HYP onset pattern; and (4) specific HFO patterns characterized these 2 types of seizure onset as ripples predominated at the onset of LVF seizures, whereas fast ripple rates were higher at the onset of HYP seizures.

Activation of the Inhibitory or Excitatory Network Can Lead to Ictal Discharges

It is well established that 4AP blocks Kv1 channels thus increasing action potential duration in both excitatory and inhibitory neurons,[19] which leads to epileptiform activity.[20] We have shown here that the EC networks under 4AP treatment can be activated by opsin stimulation in either interneurons or principal cells. However, we also discovered that activation of each specific cell population leads to ictal discharges with a different onset pattern. Namely, seizure like events with an LVF onset pattern can be triggered by interneuronal network activity, whereas triggering discharges with an HYP onset pattern requires synchronous activation of glutamatergic principal cells, as previously suggested by in vivo studies.[6,7] These results have not been reported in other in vitro models.

Several studies performed in the 1970s and 1980s have proposed that the initiation of focal seizures depends on weakening or failure of inhibition, a process that should lead to an uncontrolled increase in glutamatergic excitation.[21,22] However, subsequent in vitro and in vivo experiments have shown that GABAergic interneurons are not simply responsible for providing inhibitory control of brain networks[23]; rather, GABAergic inhibitory signals can, paradoxically, favor seizure initiation.[24–28] Strong recruitment of interneurons, and the consequent activation of postsynaptic $GABA_A$ receptors, can lead to epileptiform synchronization and ictogenesis via several mechanisms that result from intracellular Cl^- accumulation and include: (1) a positive shift in Cl^- reversal potential that makes $GABA_A$ receptor signaling excitatory[29]; and (2) an increase in extracellular $[K^+]$ that is caused by the activity of potassium chloride cotransporter-2, which extrudes both Cl^- and K^+ from the intraneuronal compartments.[30] In addition, it has been reported that excessive interneuron firing can result in depolarization block[31] and perhaps synchronize neuronal populations through rebound excitation. [25,32] Therefore, excessive activation of interneurons can very well be sufficient to disrupt the excitation/inhibition balance within the neuronal network, thus triggering ictal-like discharges.

Optogenetic Activation of PV- and SOM-Positive Interneurons Triggers LVF Onset Seizures

We have recently reported that PV interneuron activation in a constitutive model of ChR2 expression triggered LVF onset ictal discharges.[14] Here, we have confirmed the contribution of PV interneurons to LVF discharges using a novel strain with a PV-Cre background in which we provided the enhanced ChR2 opsin, ChETA, using a stereotaxic virus injection procedure. In addition, as recently reported by Yekhlef et al,[33] we found that the optogenetic activation of SOM interneurons in EC is also sufficient to trigger LVF onset events.

Because previous studies have shown that GABA application to the dendrites induces depolarizing responses, whereas its application to the soma results in hyperpolarization,[34–37] we anticipated differences in the ability of somatic-targeting PV and dendritic-targeting SOM interneurons to trigger ictal discharges in the EC network. In addition, PV interneurons innervate twice as many principal cells as other interneurons and receive more local excitatory input[38]; therefore, we expected these cells to play more preponderant roles compared to other interneuron types in triggering of ictal discharges. However, we found that activation of either fast-spiking PV cells or non–fast-spiking SOM cells are equally effective in triggering ictal discharges with an LVF onset pattern. This may be partially

explained by the finding that SOM interneurons are extensively coupled via gap junctions and fire more readily in response to convulsive agents like 4AP.[39] Also, Cl^- accumulation is greater and faster in smaller dendritic compartments in comparison to larger somas, thus allowing GABAergic activity to become depolarizing.[40] Finally, activation of both PV and SOM interneurons leads to the release of GABA, which has been shown to result in an increase in extracellular $[K^+]$ regardless of target compartments.[41]

Optogenetic Activation of CamKII-Positive Neurons Triggers HYP Onset Seizures

It has been proposed that LVF and HYP seizures depend on the activity of distinct neural networks.[4,6,42] Accordingly, we have recently reported that systemic injection of the $GABA_A$ receptor antagonist picrotoxin in vivo induces seizures characterized by an HYP onset pattern, whereas seizures induced by 4AP in these experiments are most often characterized by an LVF seizure onset pattern. [13] This evidence is in line with in vitro work performed on human tissue, where it was shown that pyramidal cell firing and therefore, glutamatergic mechanisms herald the onset of HYP seizures.[43] We have shown here that repetitive optogenetic activation of CamKII-positive principal cells in the EC is sufficient to switch the 4AP-induced LVF onset discharges to HYP onset discharges.

In line with the in vivo observations reported[6] in the pilocarpine TLE model, we found that LVF onset discharges lasted longer than HYP onset discharges. The cellular and pharmacological mechanisms responsible for such different duration remain to be elucidated; however, it has been proposed that this could result from HYP onset discharges often arising from the hippocampal region, whereas LVF onset discharges often start in parahippocampal regions including the EC.[2,4,42] Our data, obtained from the same structure, suggest that the involvement of glutamatergic signaling results in shorter periods of epileptiform synchronization. Further studies are, however, needed to confirm this hypothesis.

It is worthy to note that LVF and HYP are not the only 2 seizure onset patterns identified in TLE.[3,44–46] We also recorded spontaneous ictal events that did not clearly fall in either of these 2 categories; these ictal discharges were, however, rare and were thus excluded from our analysis, as we were interested in the mechanisms underlying LVF and HYP seizure onset patterns.

High-Frequency Oscillations Associated with LVF and HYP Onset Seizures

Evidence obtained from in vitro[47] and in vivo[6,7] animal models as well as from epileptic patients[48] indicates that HFO rate of occurrence increases shortly before the appearance of ictal activity and remains high throughout. Ripples occur when inhibitory interneurons entrain pyramidal cells and other interneurons into a rhythmic pattern of firing.[10] We found that optogenetic stimulation of interneurons that triggered LVF onset discharges were associated with higher ripple rates at onset. Fast ripples, conversely, are thought to rely on population spikes arising from hypersynchronous firing of small groups of principal neurons.[49] As expected, we found higher fast ripple rates at the onset of ictal discharges with an HYP pattern triggered by optogenetic activation of CamKII-positive principal cells in the EC. Our results therefore suggest that HFOs in different frequency bands during distinct

seizure onset patterns reflect dynamic processes that may rest on the functional organization of specific types of neuronal clusters.[5,6,8] However, further investigation is required to confirm these presumptions, because oscillatory frequency alone is not sufficient to distinguish between different pathological HFOs.[50]

Concluding Remarks

Our results demonstrate the contribution of 2 types of GABAergic interneurons to LVF onset discharges. We also discovered the ability to switch 4AP-induced LVF onset discharges to HYP discharges by optogenetic activation of a local pool of principal glutamatergic cells in EC. These findings can provide insight for clinicians to delineate better therapeutic targets in the treatment of TLE depending on seizure onset patterns and the associated HFOs. Additional studies should investigate the effect of optogenetic inhibition of these interneurons or principal cells in modulating ictal discharge progression.

Acknowledgments

This study was supported by the Canadian Institutes of Health Research (8109, 74609, M.A.; MOP119340, S.W.) and a student scholarship from the Savoy Foundation for Epilepsy (Z.S.).

References

1. Ogren JA, Wilson CL, Bragin A, et al. Three-dimensional surface maps link local atrophy and fast ripples in human epileptic hippocampus. Ann Neurol. 2009; 66:783–791. [PubMed: 20035513]
2. Velasco AL, Wilson CL, Babb TL, Engel J Jr. Functional and anatomic correlates of two frequently observed temporal lobe seizure-onset patterns. Neural Plast. 2000; 7:49–63. [PubMed: 10709214]
3. Perucca P, Dubeau F, Gotman J. Intracranial electroencephalographic seizure-onset patterns: effect of underlying pathology. Brain. 2014; 137:183–196. [PubMed: 24176980]
4. Bragin A, Azizyan A, Almajano J, Engel J. The cause of the imbalance in the neuronal network leading to seizure activity can be predicted by the electrographic pattern of the seizure onset. J Neurosci. 2009; 29:3660–3671. [PubMed: 19295168]
5. Bragin A, Engel J Jr, Wilson CL, et al. Electrophysiologic analysis of a chronic seizure model after unilateral hippocampal KA injection. Epilepsia. 1999; 40:1210–1221. [PubMed: 10487183]
6. Lévesque M, Salami P, Gotman J, Avoli M. Two seizure-onset types reveal specific patterns of high-frequency oscillations in a model of temporal lobe epilepsy. J Neurosci. 2012; 32:13264–13272. [PubMed: 22993442]
7. Bragin A, Azizyan A, Almajano J, et al. Analysis of chronic seizure onsets after intrahippocampal kainic acid injection in freely moving rats. Epilepsia. 2005; 46:1592–1598. [PubMed: 16190929]
8. Engel J Jr, Bragin A, Staba R, Mody I. High-frequency oscillations: what is normal and what is not? Epilepsia. 2009; 50:598–604. [PubMed: 19055491]
9. Jefferys JGR, Menendez de la Prida L, Wendling F, et al. Mechanisms of physiological and epileptic HFO generation. Prog Neurobiol. 2012; 98:250–264. [PubMed: 22420980]
10. Ylinen A, Bragin A, Nadasdy Z, et al. Sharp wave-associated high-frequency oscillation (200 Hz) in the intact hippocampus: network and intracellular mechanisms. J Neurosci. 1995; 15:30–46. [PubMed: 7823136]
11. Avoli M, de Curtis M. GABAergic synchronization in the limbic system and its role in the generation of epileptiform activity. Prog Neurobiol. 2011; 95:104–132. [PubMed: 21802488]
12. Lévesque M, Salami P, Behr C, Avoli M. Temporal lobe epileptiform activity following systemic administration of 4-aminopyridine in rats. Epilepsia. 2013; 54:596–604. [PubMed: 23521339]
13. Salami P, Lévesque M, Gotman J, Avoli M. Distinct EEG seizure patterns reflect different seizure generation mechanisms. J Neurophysiol. 2015; 113:2840–2844. [PubMed: 25652916]

14. Shiri Z, Manseau F, Lévesque M, et al. Interneuron activity leads to initiation of low-voltage fast-onset seizures. Ann Neurol. 2015; 77:541–546. [PubMed: 25546300]
15. DeFelipe J, Löpez-Cruz PL, Benavides-Piccione R, et al. New insights into the classification and nomenclature of cortical GABAergic interneurons. Nat Rev Neurosci. 2013; 14:202–216. [PubMed: 23385869]
16. De Guzman P, Inaba Y, Baldelli E, et al. Network hyperexcitability within the deep layers of the pilocarpine-treated rat entorhinal cortex. J Physiol. 2008; 586:1867–1883. [PubMed: 18238812]
17. McCormick DA, Connors BW, Lighthall JW, Prince DA. Comparative electrophysiology of pyramidal and sparsely spiny stellate neurons of the neocortex. J Neurophysiol. 1985; 54:782–806. [PubMed: 2999347]
18. Schwartzkroin PA. Characteristics of CA1 neurons recorded intracellularly in the hippocampal in vitro slice preparation. Brain Res. 1975; 85:423–436. [PubMed: 1111846]
19. Zhang L, McBain CJ. Potassium conductances underlying repolarization and after-hyperpolarization in rat CA1 hippocampal interneurones. J Physiol. 1995; 488:661–672. [PubMed: 8576856]
20. Smart SL, Lopantsev V, Zhang CL, et al. Deletion of the K(V)1. 1 potassium channel causes epilepsy in mice. Neuron. 1998; 20:809–819. [PubMed: 9581771]
21. Ben-Ari Y, Krnjević K, Reinhardt W. Hippocampal seizures and failure of inhibition. Can J Physiol Pharmacol. 1979; 57:1462–1466.
22. Ayala GF, Matsumoto H, Gumnit RJ. Excitability changes and inhibitory mechanisms in neocortical neurons during seizures. J Neurophysiol. 1970; 33:73–85. [PubMed: 4312440]
23. Freund TF, Buzsáki G. Interneurons of the hippocampus. Hippocampus. 1996; 6:347–470. [PubMed: 8915675]
24. Avoli M, Barbarosie M, Lücke A, et al. Synchronous GABA-mediated potentials and epileptiform discharges in the rat limbic system in vitro. J Neurosci. 1996; 16:3912–3924. [PubMed: 8656285]
25. Gnatkovsky V, Librizzi L, Trombin F, de Curtis M. Fast activity at seizure onset is mediated by inhibitory circuits in the entorhinal cortex in vitro. Ann Neurol. 2008; 64:674–686. [PubMed: 19107991]
26. Grasse DW, Karunakaran S, Moxon KA. Neuronal synchrony and the transition to spontaneous seizures. Exp Neurol. 2013; 248:72–84. [PubMed: 23707218]
27. Schevon CA, Weiss SA, McKhann G, et al. Evidence of an inhibitory restraint of seizure activity in humans. Nat Commun. 2012; 3:1060. [PubMed: 22968706]
28. Truccolo W, Donoghue JA, Hochberg LR, et al. Single-neuron dynamics in human focal epilepsy. Nat Neurosci. 2011; 14:635–641. [PubMed: 21441925]
29. Khalilov I, Le Van Quyen M, Gozlan H, Ben-Ari Y. Epileptogenic actions of GABA and fast oscillations in the developing hippocampus. Neuron. 2005; 48:787–796. [PubMed: 16337916]
30. Viitanen T, Ruusuvuori E, Kaila K, Voipio J. The K+-Cl cotransporter KCC2 promotes GABAergic excitation in the mature rat hippocampus. J Physiol. 2010; 588(pt 9):1527–1540. [PubMed: 20211979]
31. Ziburkus J, Cressman JR, Barreto E, Schiff SJ. Interneuron and pyramidal cell interplay during in vitro seizure-like events. J Neurophysiol. 2006; 95:3948–3954. [PubMed: 16554499]
32. Jefferys, JGR., Jiruska, P., de Curtis, M., Avoli, M. Limbic network synchronization and temporal lobe epilepsy. In: Noebels, JL.Avoli, M.Rogawski, MA., et al., editors. Jasper's basic mechanisms of the epilepsies. Bethesda, MD: US National Center for Biotechnology Information; 2012. Available at: http://www.ncbi.nlm.nih.gov/books/NBK98158/ [Accessed January 17, 2014]
33. Yekhlef L, Breschi GL, Lagostena L, et al. Selective activation of parvalbumin- or somatostatin-expressing interneurons triggers epileptic seizure like activity in mouse medial entorhinal cortex. J Neurophysiol. 2015; 113:1616–1630. [PubMed: 25505119]
34. Alger BE, Nicoll RA. Pharmacological evidence for two kinds of GABA receptor on rat hippocampal pyramidal cells studied in vitro. J Physiol. 1982; 328:125–141. [PubMed: 7131310]
35. Andersen P, Dingledine R, Gjerstad L, et al. Two different responses of hippocampal pyramidal cells to application of gamma-amino butyric acid. J Physiol. 1980; 305:279–296. [PubMed: 7441554]

36. Misgeld U, Deisz RA, Dodt HU, Lux HD. The role of chloride transport in postsynaptic inhibition of hippocampal neurons. Science. 1986; 232:1413–1415. [PubMed: 2424084]
37. Perreault P, Avoli M. Physiology and pharmacology of epileptiform activity induced by 4-aminopyridine in rat hippocampal slices. J Neurophysiol. 1991; 65:771–785. [PubMed: 1675671]
38. Krook-Magnuson E, Armstrong C, Oijala M, Soltesz I. On-demand optogenetic control of spontaneous seizures in temporal lobe epilepsy. Nat Commun. 2013; 4:1376. [PubMed: 23340416]
39. Lillis KP, Kramer MA, Mertz J, et al. Pyramidal cells accumulate chloride at seizure onset. Neurobiol Dis. 2012; 47:358–366. [PubMed: 22677032]
40. Ellender TJ, Raimondo JV, Irkle A, et al. Excitatory effects of parvalbumin-expressing interneurons maintain hippocampal epileptiform activity via synchronous afterdischarges. J Neurosci. 2014; 34:15208–15222. [PubMed: 25392490]
41. Barolet AW, Morris ME. Changes in extracellular K+ evoked by GABA, THIP and baclofen in the guinea-pig hippocampal slice. Exp Brain Res. 1991; 84:591–598. [PubMed: 1650707]
42. Memarian N, Madsen SK, Macey PM, et al. Ictal depth EEG and MRI structural evidence for two different epileptogenic networks in mesial temporal lobe epilepsy. PLoS One. 2015; 10:e0123588. [PubMed: 25849340]
43. Huberfeld G, Menendez de la Prida L, Pallud J, et al. Glutamatergic pre-ictal discharges emerge at the transition to seizure in human epilepsy. Nat Neurosci. 2011; 14:627–634. [PubMed: 21460834]
44. Pacia SV, Ebersole JS. Intracranial EEG substrates of scalp ictal patterns from temporal lobe foci. Epilepsia. 1997; 38:642–654. [PubMed: 9186246]
45. Alarcon G, Binnie CD, Elwes RD, Polkey CE. Power spectrum and intracranial EEG patterns at seizure onset in partial epilepsy. Electroencephalogr Clin Neurophysiol. 1995; 94:326–337. [PubMed: 7774519]
46. Wetjen NM, Marsh WR, Meyer FB, et al. Intracranial electroencephalography seizure onset patterns and surgical outcomes in nonlesional extratemporal epilepsy. J Neurosurg. 2009; 110:1147–1152. [PubMed: 19072306]
47. Khosravani H, Pinnegar CR, Mitchell JR, et al. Increased high-frequency oscillations precede in vitro low-Mg seizures. Epilepsia. 2005; 46:1188–1197. [PubMed: 16060927]
48. Zijlmans M, Jacobs J, Zelmann R, et al. High frequency oscillations and seizure frequency in patients with focal epilepsy. Epilepsy Res. 2009; 85:287–292. [PubMed: 19403269]
49. Jiruska P, Finnerty GT, Powell AD, et al. Epileptic high-frequency network activity in a model of non-lesional temporal lobe epilepsy. Brain J Neurol. 2010; 133(pt 5):1380–1390.
50. Menendez de la Prida L, Trevelyan AJ. Cellular mechanisms of high frequency oscillations in epilepsy: on the diverse sources of pathological activities. Epilepsy Res. 2011; 97:308–317. [PubMed: 21482073]

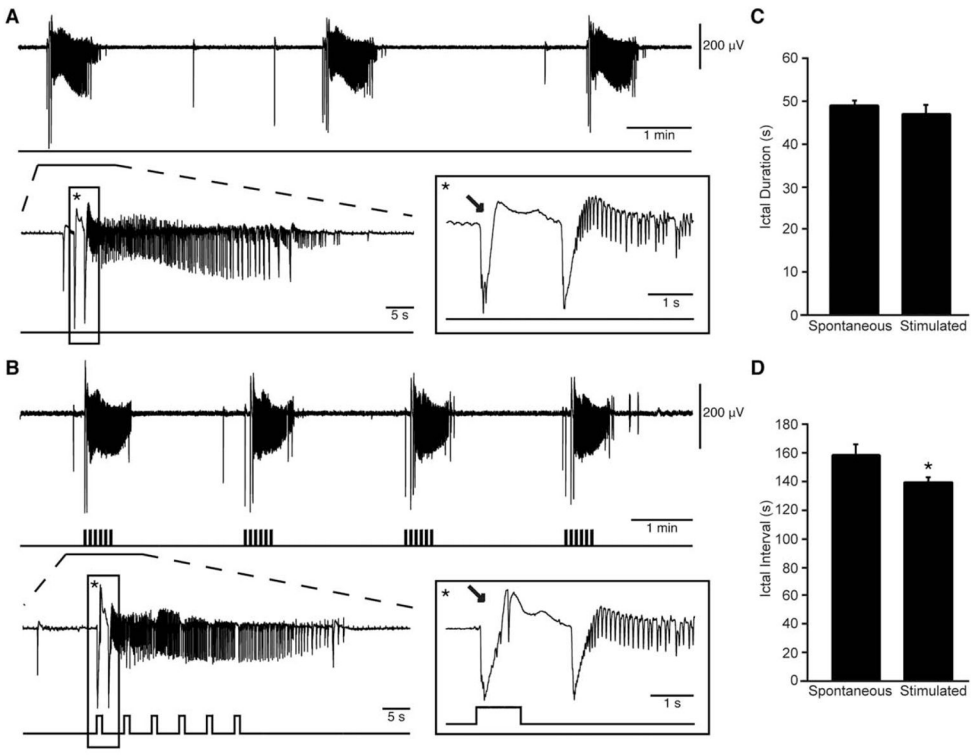

FIGURE 1.

Low-voltage, fast ictal discharges can occur spontaneously or be triggered by optogenetic activation of parvalbumin interneurons. (A) Spontaneous ictal discharges occurring during bath application of 4-aminopyridine (4AP); 1 event is further expanded to show the onset pattern *(asterisk)*. (B) Ictal discharges evoked by 1-second light pulses at 0.2Hz during bath application of 4AP; 1 of these events is further expanded to compare the onset patterns *(asterisk)*. Note that in both A and B, the ictal discharge is preceded by 1 or 2 negative-going interictal field potentials *(arrows)*. (C, D) Quantification of the duration and interval of occurrence of the spontaneous and stimulated ictal events recorded in these experiments (*$p < 0.05$).

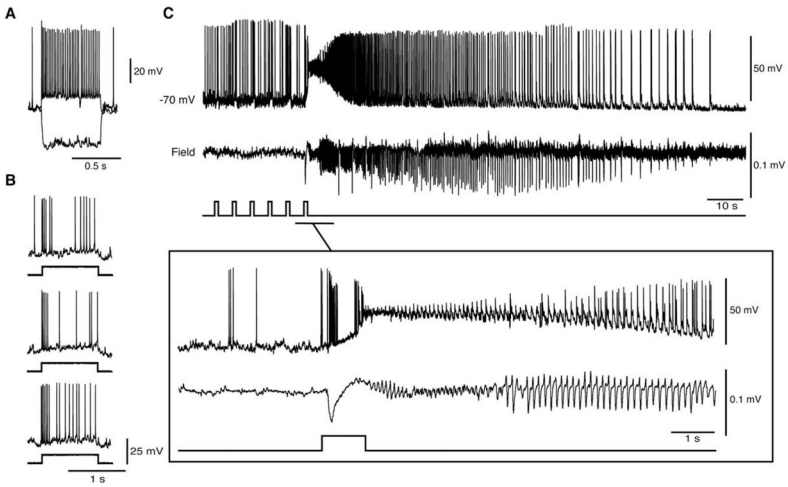

FIGURE 2.

Optogenetic activation of parvalbumin (PV) interneurons in the whole-cell configuration triggers low-voltage, fast (LVF) ictal discharges. (A) Electrophysiological characterization of an entorhinal cortex fast-spiking PV interneuron during injection of hyperpolarizing and depolarizing current pulses (membrane potential [peak velocity]=−70mV; parameters of the intracellular current pulses=600 milliseconds, −200 and 160pA; membrane resistance=121MΩ; access resistance=36MΩ). (B) Responses generated by the same cell as in A to 1-second light pulses delivered at 3-minute intervals. Note that similar action potential discharges are generated over time. (C) Optogenetic activation of this interneuron (and of the concomitant LVF ictal discharge) by a train of 1-second light pulses at 0.2Hz. The onset of the ictal event is expanded below to further reveal the LVF pattern.

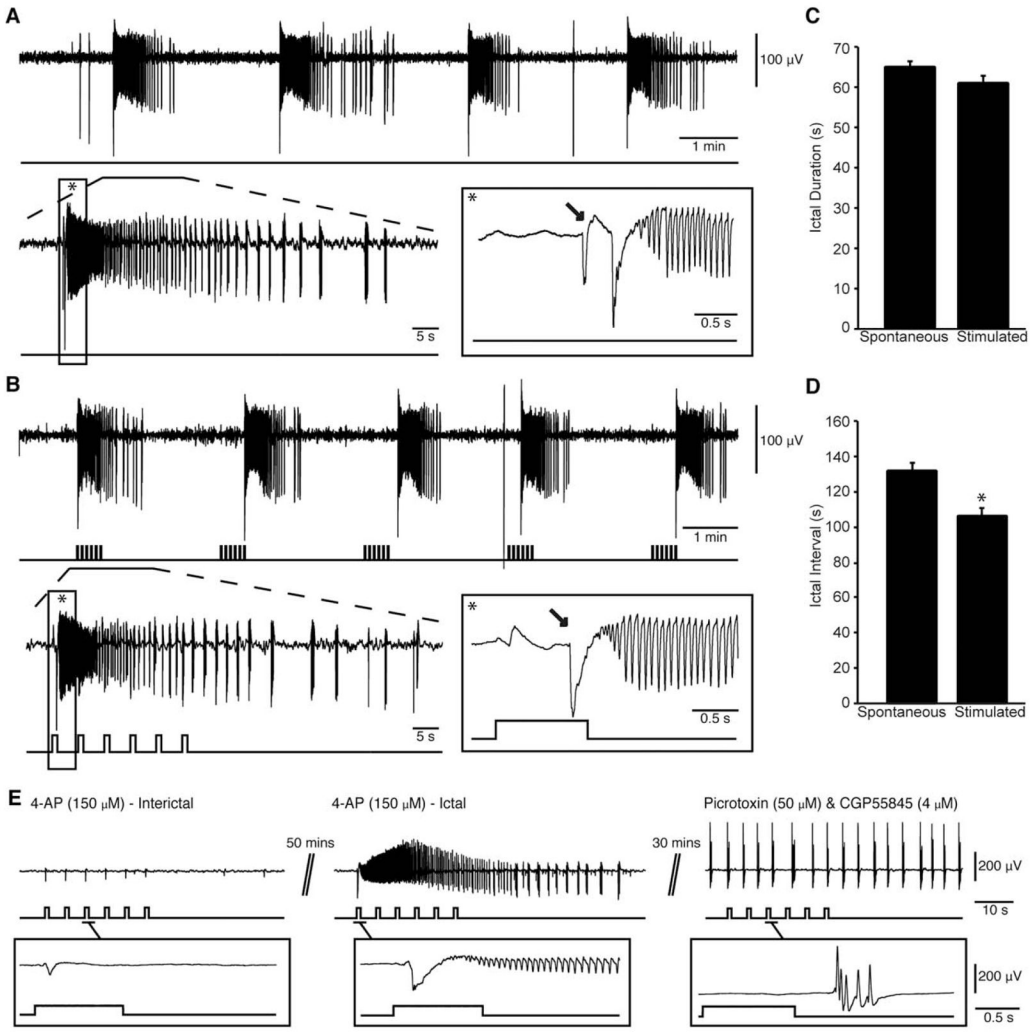

FIGURE 3.

Low-voltage, fast ictal discharges can also be triggered by optogenetic activation of somatostatin interneurons. (A) Spontaneous ictal discharges occurring during bath application of 4-aminopyridine (4AP); 1 of the events is further expanded to show the onset pattern *(asterisk)*. (B) Ictal discharges evoked by a 30-second train of 1-second light pulses at 0.2Hz during bath application of 4AP; 1 of the events is further expanded to compare the onset patterns *(asterisk)*. Note that in both A and B, ictal discharges are preceded by 1 or 2 negative-going interictal field potentials *(arrows)*. (C, D) Duration and interval of occurrence of spontaneous and stimulated ictal events are quantified (*$p < 0.05$). Note that we were able to trigger ictal discharges at higher frequencies than what occurs spontaneously. (E) Example 4AP-induced interictal discharges and ictal discharge triggered by trains of 1-second light pulses; bath application of 50 μM picrotoxin and 4 μM CGP55845 blocked all ictal discharges and responses to stimuli (see expanded example).

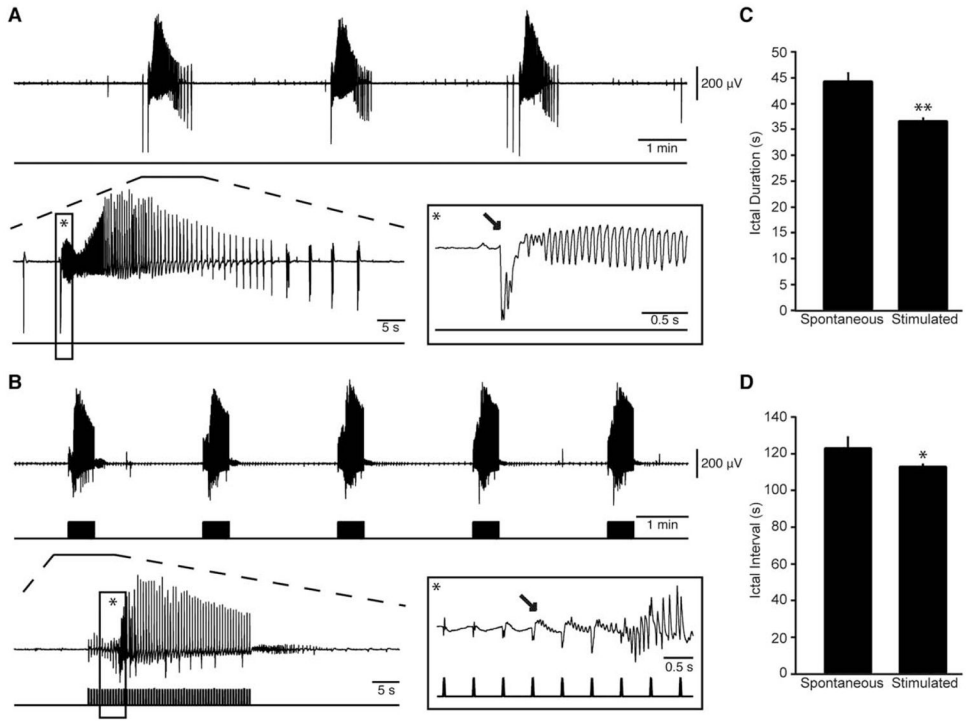

FIGURE 4.

Hypersynchronous (HYP) ictal discharges can be triggered by optogenetic activation of calmodulin-dependent protein kinase principal neurons. (A) Spontaneous ictal discharges occurring during bath application of 4-aminopyridine (4AP); 1 of the events is further expanded to show the onset pattern *(asterisk)*. (B) Ictal discharges evoked by 20-millisecond light pulses at 2Hz during bath application of 4AP; 1 of these events is further expanded to compare the onset pattern *(asterisk)*. Note that in B, the ictal discharge is preceded by repeated spiking that is characteristic of HYP seizure onset (1 of these spikes is indicated by an *arrow*). (C, D) Plots of the duration and interval of occurrence of spontaneous and stimulated ictal events. Note that the stimulated HYP onset discharges were shorter than the spontaneous low-voltage, fast discharges (*$p < 0.05$, **$p < 0.01$).

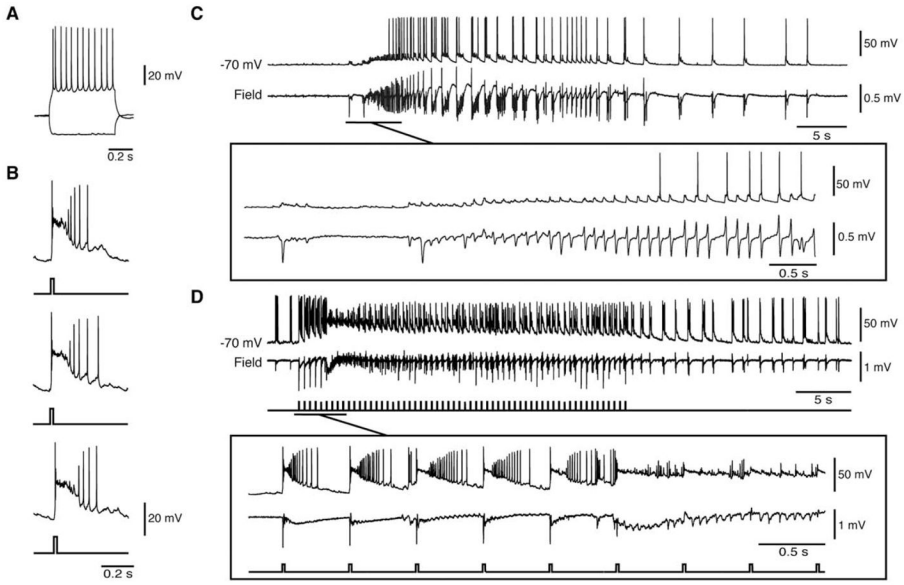

FIGURE 5.

Optogenetic activation of calmodulin-dependent protein kinase (CamKII) principal cells in the whole-cell configuration triggers hypersynchronous (HYP) ictal discharges. (A) Electrophysiological characterization of an entorhinal cortex CamKII neuron during injection of hyperpolarizing and depolarizing current pulses (peak velocity=−70mV; characteristics of the intracellular current pulses=600 milliseconds, −200 and 160pA; membrane resistance=87MΩ; access resistance=26MΩ). (B) Successive responses to 20-millisecond light pulses recorded from the same cell at 3-minute intervals. Note that similar action potential discharges are generated over time. (C) Firing pattern of a principal cell during a 4-aminopyridine–induced spontaneous low-voltage, fast (LVF) onset ictal discharge. Note that the principal cell is quiescent at the onset of the LVF discharge. (D) Optogenetic activation of a CamKII-positive neuron (and of the concomitant HYP ictal discharge) by a train of 20-millisecond light pulses at 2Hz. The onset of the ictal event is expanded below to further reveal the HYP pattern.

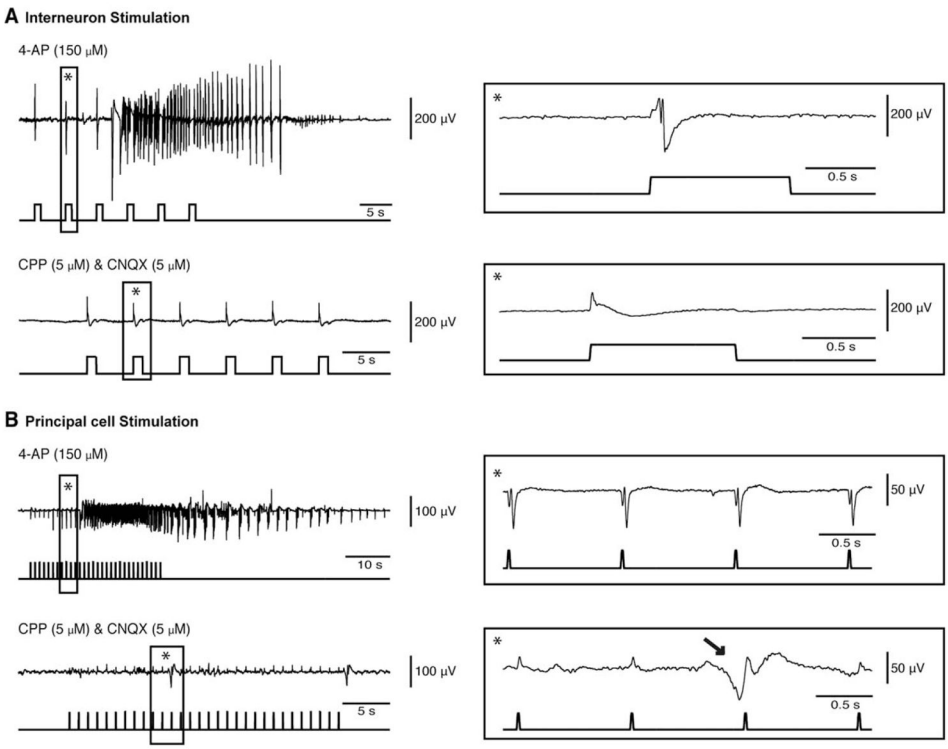

FIGURE 6.

Blockade of glutamatergic neurotransmission abolishes both spontaneously occurring and optogenetically induced ictal events. (A) Example of an ictal discharge induced by a train of 1-second light pulses at 0.2Hz that activate parvalbumin-positive interneurons in the entorhinal cortex (EC) during bath application of 4-aminopyridine (4AP); a light-induced interictal discharge is expanded on the right *(asterisk)*. Note that bath application of 5μM 3-([*R*]-2-carboxypiperazin-4-yl)-propyl-1-phosphonic acid (CPP) and 5μM 6-cyano-7-nitroquinoxaline-2,3-dione (CNQX) block all ictal discharges, whereas light-driven presumptive γ-aminobutyric acidergic (GABAergic) interictal events could be still evoked. (B) Example of an ictal discharge induced by a train of 20-millisecond light pulses at 1Hz activating calmodulin-dependent protein kinase–positive principal cells in the EC during bath application of 4AP; part of the trace is further expanded to show the direct responses to stimuli *(asterisk)*. In this experiment as well, bath application of 5μM CPP and 5μM CNQX abolishes spontaneous and light-induced ictal discharges; under these condition, spontaneous GABAergic discharges could, however, be recorded *(arrow)*. Note that the small deflections in the field potential trace coinciding with stimuli are stimulation artifacts.

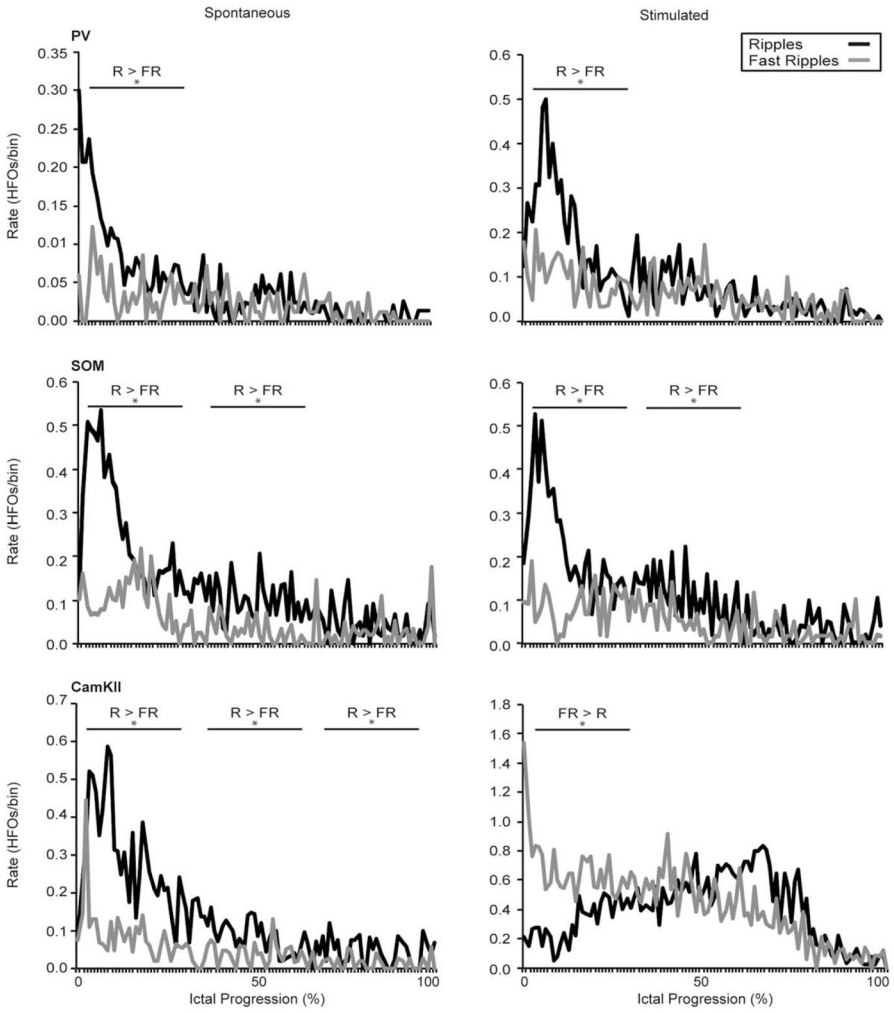

FIGURE 7.

Specific patterns of high-frequency oscillations (HFOs) characterize low-voltage, fast (LVF) and hypersynchronous (HYP) onset ictal discharges. Average rate of ripples (R) and fast ripples (FR) are plotted over time for spontaneous 4-aminopyridine–induced (left) and optogenetically stimulated (right) ictal discharges in parvalbumin (PV), somatostatin (SOM), and calmodulin-dependent protein kinase (CamKII) slices (n=10 events for each plot). Wideband recordings of spontaneous and stimulated ictal discharges were filtered to detect HFOs throughout the event from the onset (0% progression) to the end of the ictal discharge (100% progression). Note that ripple rates predominate in the LVF onset discharges, whereas fast ripple rates are higher at the onset of HYP discharges triggered by CamKII-cell stimulation (*$p < 0.01$).